Available online at www.sciencedirect.com
ScienceDirect
Journal of Nuclear Materials 362 (2007) 374–382
journal of nuclear materials
www.elsevier.com/locate/jnucmat

Prediction of oxygen potential in americium thorium oxides phase of a cermet fuel

M. Osaka [a,*], K. Kurosaki [b], S. Yamanaka [b]

[a] Japan Atomic Energy Agency, Narita-cho 4002, Oarai-machi, Higashiibaraki-gun, Ibaraki 311-1393, Japan
[b] Division of Sustainable Energy and Environmental Engineering, Graduate School of Engineering, Osaka University, Yamadaoka 2-1, Suita-shi, Osaka 565-0871, Japan

Abstract

Prediction of the oxygen potential variation during burnup for ThO_2-based Am-containing cermet fuel, which consists of $(Am,Th)O_{2-x}$ host phase and molybdenum inert matrix, in a fast reactor was carried out by the chemical thermodynamic method. The oxygen potentials of $(Eu,U)O_{2-x}$ and $(Pu,Th)O_{2-x}$ were analyzed and related thermodynamic data were obtained. These data, together with those in the literature for the components in the burnup fuel, were used for oxygen potential prediction during burnup considering the oxygen and metal balances. It was revealed that the addition of a small amount of depleted-U to the host phase of the fuel effectively lowered the high oxygen potential observed at the initial stage of the burnup.

PACS: 28.41.Bm

1. Introduction

Recycling and transmutation of minor actinides (MAs), which are recovered from spent nuclear fuel, in fast reactors (FRs) are the key processes for the successful realization of the FR-based nuclear fuel cycle in Japan [1], together with MA- and Pu-recycling and transmutation in the existing LWRs as inert matrix fuel [2,3]. The most promising candidate fuel for such FRs is considered to be the mixed oxide (MOX) fuel of U and Pu with several percent of MAs and fission products (FPs) [4]. The MA content in the MOX fuel varies mainly according to the required mass-balance for MAs. It would reach an equilibrium value of about 1% if the steady-state operation of the FR-based cycle is realized in the future. On the other hand, the MAs should be transmuted as soon as possible since a great amount of MAs has already been accumulated even in the present nuclear park. For this purpose, the MA content in the MOX fuel should be raised, especially in the introductory phase of the FR.

For oxide fuel, oxygen potential is one of the most important properties that affect almost all aspects of fuel behaviors. In particular, aspects of

* Corresponding author. Tel.: +81 29 267 4141; fax: +81 29 266 0016.
E-mail address: ohsaka.masahiko@jaea.go.jp (M. Osaka).

0022-3115/$ - see front matter © 2007 Elsevier B.V. All rights reserved.
doi:10.1016/j.jnucmat.2007.01.083

cladding corrosion and oxidation during burnup are significantly affected by the oxygen potential of the fuel. It is reported that the oxygen potentials of Am-containing UO_2-based fuels with a fluorite structure are high [5,6], while those of Np-containing UO_2-based fuel are at the same level as those of MOX [7]. Although the oxygen potential of Am-containing UO_2-based fuels can be reduced by a lowering of the O/M ratio, it could cause other significant problems, especially in terms of thermal performances of the fuel [8,9]. Alternative Am-containing fuels should, therefore, be developed.

The authors have proposed a composite fuel for Am transmutation in order to overcome the problems caused by high oxygen potential [10]. Table 1 lists the fundamental specifications of this fuel. The fuel is composed of micro- or macro-spheres of $(Am,Th)O_{2-x}$ dispersed in a molybdenum (Mo) inert matrix (IM). Although such concepts as the combination of oxide-spheres and metal-IM (cermet) have been studied for a long time, not only as fuel with high thermal performance [11,12] but also as the inert matrix fuels including MAs, e.g. [13,14], a new idea, namely the use of recovered Mo from spent nuclear fuel as the IM, has been envisaged in this fuel for the reduction and effective utilization of radioactive waste.

The detailed concept of this fuel has been described in Ref. [10]. The deployment of ThO_2 as the diluent of AmO_{2-x} is mainly due to its stability with the fluorite structure. This structure represents nuclear fuel mainly because of its structural advantages, i.e., isotropy, high metal density, high melting temperature and thermal conductivity, sufficient space for FP-inclusion, and so on. Americium tends to be present as sesquioxide because of its trivalent state stability [15,16]. It is expected that americium oxide is soluble in thorium dioxide within the fluorite structure. The enhancement of the thermal properties of the Am-oxides by ThO_2 [17] are also favorable. ThO_2-based fuel also indicates some neutronic advantages over UO_2-based fuel, i.e., yielding a new fissile material of ^{233}U and suppressing the newly generating MAs by burnup [18]. Molybdenum is considered to be one of the most promising IMs mainly owing to its high melting temperature, good thermophysical and mechanical properties and high adaptability to the traditional powder metallurgical fabrication procedure [19,20]. In addition, Mo is expected to suppress any increase in the oxygen potential during burnup by taking up the excess oxygen resulting from the dissolution and precipitation of FP elements. Consequently, the oxygen potential of a system including an appropriate amount of Mo is expected to be maintained at an appropriate level throughout the burnup. Previous considerations [10] showed that the addition of 10% of Mo is sufficient for both the suppression of oxygen potential increase during the burnup and enhancement of the thermal conductivity. The lower Mo content is also preferred in terms of its smaller impact on the core characteristics.

Table 1
Fundamental specifications of the ThO_2-based Am-containing cermet fuel

Fuel form	• Sintered columnar pellet • Two phases of host and IM phases • Homogeneous dispersion of host spheres into IM
Host phase	• $(Am_yTh_{1-y})O_{2-x}$ solid solution with $y < 0.5$ • Macro spheres having diameters up to 300 μm or micro ones
Inert matrix (IM)	• Recovered molybdenum from spent fuel • Weight ratio of the Mo-IM: 0.1 to 0.5

One critical problem for this fuel is the high absorption cross-section of the recovered Mo in a fast neutron spectrum, which can cause problems for the FR core characteristics. The use of Mo enriched with ^{92}Mo is, therefore, considered in the fuel for an accelerator driven sub-critical system [21]. This problem is, however, expected to be solved if an optimum core loading of the fuel is made [10]. Nevertheless, various properties and related behaviors should be evaluated for a successful realization of this fuel.

In this paper, variation of the oxygen potential of this fuel during burnup in a FR is estimated by the chemical thermodynamic method. Analyses of the oxygen potentials of $(Eu,U)O_{2-x}$ and $(Pu,Th)O_{2-x}$ are carried out for this purpose. Appropriate compositions of the fuel are also discussed in terms of the optimization of the oxygen potential.

2. Oxygen potential prediction

In this section, variation of the oxygen potential of the fuel during burnup in a FR is estimated by means of the chemical thermodynamic method proposed by Lindemer and Besmann [22]. The estimation is made on the host phase of the fuel, $(Am,Th)O_{2-x}$. This is because the host phase dominates the oxygen potential of the system, while the Mo-IM only functions as an oxygen getter.

2.1. General description of the chemical thermodynamic method

In the chemical thermodynamic method proposed by Lindemer and Besmann [22], the non-stoichiometric oxide is considered to be a solid solution of two or more assumed stoichiometric species. For example, PuO_{2-x} is assumed to be a solid solution of Pu_2O_3 and PuO_2. Interactions expressed as the Redlich–Kister polynomial [23] between two specific species are usually introduced, which leads to a better representation. It is of note that stoichiometric compositions for these species are not limited to integer values as long as the elemental ratios in the species are maintained. This is done for the better representation of the experimental data. The species is, therefore, called the 'mass parameter' in this method. The Gibbs formation energy for the non-stoichiometric oxide is, thus, expressed by the following equation, for the PuO_{2-x} case as an example [24].

$$\begin{aligned}\frac{\Delta G_f^0\langle PuO_{2-x}\rangle}{m} &= N_{Pu_{4/3}O_2}\Delta G_f^0\langle Pu_{4/3}O_2\rangle \\ &+ N_{PuO_2}\Delta G_f^0\langle PuO_2\rangle \\ &+ N_{Pu_{4/3}O_2}RT\ln[N_{Pu_{4/3}O_2}] \\ &+ N_{PuO_2}RT\ln[N_{PuO_2}] \\ &+ N_{Pu_{4/3}O_2}N_{PuO_2}E, \end{aligned} \quad (1)$$

where $\Delta G_f^0\langle i\rangle$ is the standard Gibbs energy of formation for mass parameter i, N_i is the mole fraction of mass parameter i, m is the sum of moles of all mass parameters, and E is the interaction energy for the first term of the polynomial [23].

A continuous change of non-stoichiometry is expressed by a corresponding continuous compositional change of each mass parameter. The oxygen partial pressure over a solid solution at a specific non-stoichiometry is expressed by an appropriate gas–solid reaction between mass parameters. The following reaction has been introduced for the PuO_{2-x} case [24].

$$3[Pu_{4/3}O_2] + (O_2) \leftrightarrow 4[PuO_2]. \quad \{1\}$$

Gibbs energy relation for Reaction {1} can be drawn as follows.

$$RT\ln(p_{O_2}^*) = 4\Delta\overline{G}[PuO_2] - 3\Delta\overline{G}[Pu_{4/3}O_2], \quad (2)$$

where $\Delta\overline{G}[i]$ is the partial molar Gibbs formation energy for the mass parameter i. It is associated with Eq. (1) by differentiating $m\cdot\Delta G_f^0\langle PuO_{2-x}\rangle$ by m_i, where m_i is the moles of the mass parameter i. Finally, Eq. (2) can be expressed as a function of x and T with the constants of standard Gibbs energies of formation and interaction energies by introducing the mass balance equations for each mass parameter. Actual values for the standard Gibbs energies of formation for mass parameters and interaction energies are obtained by the least square fitting of Eq. (2) to the experimental oxygen potential data. Consequently, calculation of the oxygen potentials of a non-stoichiometric phase can be reduced to the chemical thermodynamic issue for the system composed of mass parameters and oxygen gas.

So far, the following systems have been analyzed and represented by this method: UO_{2+x} [22], PuO_{2-x} [24], $(Pu,U)O_{2\pm x}$ [24], $(RE,U)O_{2\pm x}$ [25,26], AmO_{2-x} [27], CeO_{2-x} [28], $(Am,U)O_{2-x}$ [29] and $(Am,Pu,U)O_{2-x}$ [29]. The oxygen potential of multi-elemental systems can be calculated by the Gibbs energy minimization method with thermodynamic data for the components. For instance, the oxygen potential of irradiated UO_2-based fuel can be estimated with the above mentioned thermodynamic data.

2.2. Metal and oxygen balances during burnup

Compositional changes of metals and oxygen in the host phase during burnup should be precisely calculated for the estimation of oxygen potential variation. The changes for metals are calculated by the ORIGEN2 code [30] with a nuclear data library prepared for commercial FRs [31]. In this study, a case in which the fuel is loaded in the radial blanket region of a commercial FR core [32] is assumed because of its rather low impact on the core characteristics. Burnup of the fuel is calculated considering the average neutron flux in this region, $4.0\times10^{14}\ cm^{-2}\ s^{-1}$ [32].

On the other hand, the phase relation of the burnup host phase should be taken into consideration for the compositional change of oxygen (oxygen balance). The oxygen balance is calculated considering the distribution of oxygen to each phase formed in the burnup host phase. The oxygen balance is, thus, closely related to the chemical states of FPs.

Since the main component of the host phase is ThO_2, namely 70% of the initial composition, the irradiated host phase is assumed to be a ThO_2-based system, in which other actinide (AmO_2, UO_2, etc.) and FP (Nd_2O_3, CeO_2, etc.) oxides are dissolved. Consideration of the phase relationships was,

therefore, carried out based on a series of studies for burnup simulated ThO_2 and $(U,Th)O_2$ fuels performed by Ugajin et al. [33–35]. The simulated burnup in the fuel was 21.5 at.% at maximum. According to their results, the phase relationships in ThO_2-based fuels are similar to those in the UO_2-based fuel. Namely, there are fuel matrix, oxide precipitate, and metallic precipitate phases in the ThO_2-based fuels. Only Sr and Zr have different behaviors from those in the UO_2-based oxide; i.e., they do not dissolve into the fuel matrix phase as is the case for UO_2-based fuel.

Table 2 shows the resultant categorization of the burnup host phase for the present fuel. The oxygen potential of the fuel matrix phase is evaluated, as it dominates the oxygen potential of the system. The other phases are considered only for the oxygen balance calculation. Namely, oxygen is assumed to be consumed by the components of the oxide precipitate phase prior to those of the fuel matrix phase. Cesium is a volatile element and forms various compounds with other components, which subsequently do not dissolve into the fuel matrix phase. Although its behavior is not completely understood, Cs is assumed to form a mono-oxide and is categorized into the oxide precipitate phase. Although the chemical state of molybdenum varies according to the oxygen potential and burnup [36], this element is assumed to exist as an individual metallic phase.

UO_2 and PuO_2 are known to form solid solutions with ThO_2 in a wide range of mutual solubility. There are many intensive studies on the phase relations of $(RE,Th)O_{2-x}$, e.g., Refs. [37,38]. These results showed that, at high temperatures, RE elements can dissolve extensively into ThO_2. For example, the maximum solubility of Nd is greater than 60 at.% at 1823 K, followed by Pr with 57 at.%. Analogous to these aspects, MAs are assumed to dissolve into the fuel matrix phase. Specifically, Am and Cm, which have a similar stable valence state of trivalence in the oxide to those of REs, are analogous to REs, while Pa and Np, which have both tetravalent and pentavalent states, are analogous to U.

Table 2
Categorization of the burnup host phase of the fuel

Phase	Component elements
Fuel matrix	Actinide: Th, Pa, U, Np, Pu, Am, Cm Rare-earth: La, Nd, Pm, Sm, Gd, Tb, Dy, Ho, Er, Tm, Yb, Lu, Eu, Ce, Pr, Y
Oxide precipitate	Alkaline-earth: Sr, Ba Alkali: Cs Others: Zr
Metal	Mo

Thus, the compositional changes of metals and oxygen, which correspond to the change of the O/M ratio of the fuel matrix phase with burnup, can be calculated.

2.3. Thermodynamic data for the burnup host phase

In this study, the fuel matrix phase is assumed to be a solid solution that consists of ThO_2 solvent and solutes of FP and actinide oxides for the chemical thermodynamic representation. As there are a number of elements existing in the fuel matrix phase, as shown in Table 2, thermodynamic data of all the components with all possible interactions between them should be prepared for the strictest evaluation of the oxygen potential. However, it is neither rational nor realistic to do so because oxygen potentials of different oxides frequently give the same values. For instance, the oxygen potentials of $(Gd,U)O_{2-x}$ and $(Nd,U)O_{2-x}$ with the same RE contents are largely the same [39,40]. Many elements present in the fuel matrix phase can, thus, be categorized into a few elemental groups in terms of their oxygen potentials. The fuel matrix phase is, thus, assumed to consist of the following eight elemental groups, as shown in Table 3 [41,42]; i.e., U, Pu, Am, RE, Eu, Ce, Zr and Th. The fraction of each elemental group is the sum of fractions of the included elements.

The most important matter for the good representation of the fuel matrix phase, namely the multi-elemental system, is to introduce appropriate interactions. In the case of UO_2-based systems, the thermodynamic data estimated for various UO_2-based systems including appropriate interactions have already been obtained [22,24–29]. The fact that the oxygen potentials of a burnup simulated MOX fuel [43] can be expressed by this method with these thermodynamic data (Fig. 1) indicates the appropriateness of the present method for the representation of the UO_2-based systems. Although the present estimation is made for a ThO_2-based system, these UO_2-based data are also useful as U is generated from Th by the burnup, or included in the initial fuel, as will be mentioned later.

Appropriate interactions between ThO_2 and other oxides should, therefore, be considered in

Table 3
Thermodynamic data for components of the burnup fuel matrix phase

Elemental group	Component elements	Mass parameter	ΔH_f^0 (J mol^{-1})	ΔS_f^0 (J K^{-1} mol^{-1})	Reference
(a) Gibbs energy of formation for mass parameters					
U	U, Np	$[UO_2]$	−1 080 000	−169	[22]
		$[U_2O_5]$	−2 328 300	−415.3	[26]
Pu	Pu	$[Pu_{4/3}O_2]$	−1 091 900	−169.7	[25]
		$[PuO_2]$	−1 047 800	−187.7	[24]
Am	Am, Cm	$[Am_{4/s1}O_{6/s1}]$[a]	−3 530 901/$s1$	−657.9/$s1$	[27]
		$[Am_{4/3}U_{4/3}O_{16/3}]$	−2 822 000	−469	[29]
		$[AmO_2]$	−924 068	−167.47	[27]
RE	La, Nd, Pm, Sm, Gd, Tb, Dy, Ho, Er, Tm, Yb, Lu, Y	$[Ln_{4/3}O_2]$	−1 207 000	−189	[26]
		$[Ln_{2/3}U_{2/3}O_{8/3}]$	−1 449 100	−240	[26]
Eu	Eu	$[Eu_2O_3]$	−1 657 020	−313	[41]
		$[Eu_6U_{10}O_{31}]$	−15 742 911	−2229.8	
Ce	Ce, Pr	$[Ce_{4/s2}O_{6/s2}]$[b]	−3 361 100/$s2$	−472.55/$s2$	[28]
		$[CeO_2]$	−1 087 450	−209.08	[28]
Zr	Zr	$[ZrO_2]$	−1 095 443	−185.65	[41]
Th	Th	$[ThO_2]$	−1 221 529	−183.38	[42]

Interaction	ΔH_E (J mol^{-1})	ΔS_E (J K^{-1} mol^{-1})	Reference
(b) Interaction energies			
$[UO_2] \Longleftrightarrow [Am_{4/3}U_{4/3}O_{16/3}]$, 1st	366 723	210	[29]
$[UO_2] \Longleftrightarrow [Am_{4/3}U_{4/3}\ O_{16/3}]$, 2nd	−749 433	−548	[29]
$[Am_{4/s1}O_{6/s1}]$[a] $\Longleftrightarrow [Am_{4/3}U_{4/3}O_{16/3}]$, 1st	−305 711	−184	[29]
$[Am_{4/s1}O_{6/s1}]$[a] $\Longleftrightarrow [Am_{4/3}U_{4/3}O_{16/3}]$, 2nd	442 627	342	[29]
$[Pu_{4/3}O_2] \Longleftrightarrow [PuO_2]$, 2nd	−41 510	−30.2	[25]
$[Ce_{4/s2}O_{6/s2}]$[b] $\Longleftrightarrow [CeO_2]$, 1st	−70 210	−32.05	[28]
$[Ce_{4/s2}O_{6/s2}]$[b] $\Longleftrightarrow [\ CeO_2]$, 2nd	−63 765	−32.05	[28]
$[Ce_{4/s2}O_{6/s2}]$[b] $\Longleftrightarrow [\ UO_2]$, 1st	16 170	0	[25]
$[UO_2] \Longleftrightarrow [U_2O_5]$, 2nd	41 400	−38.1	[26]
$[ThO_2] \leftrightarrow [PuO_2]$ and $[AmO_2] \leftrightarrow [PuO_2]$, 1st	−10 815.1	0.39	

[a] $s1 = 2$ for $(Am, Pu, U)O_{2-x}$ and $s1 = 6$ for $(Am,U)O_{2-x}$.
[b] $s2 = 2 + 3 \times z$, where z is cerium content.

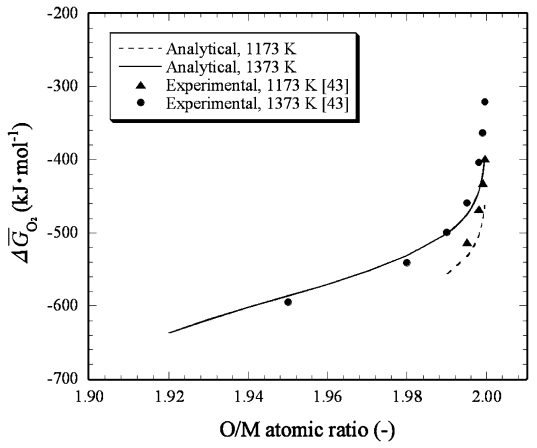

Fig. 1. Chemical thermodynamic representation of a burnup simulated MOX fuel [43].

the present evaluation. Concerning U-oxides, $(U,Th)O_{2-x}$ is reported to be the ideal solid solution of U-oxides and Th-oxide in terms of oxygen potential [44]. Namely, oxygen potentials of $(U,Th)O_{2-x}$ can be represented without any interactions between mass parameters of U-oxides and that of Th-oxide. Protactinium and Np are considered to belong to the U elemental group because of similar variable valence states, as mentioned above.

On the other hand, there exists a small deviation from the ideal for $(Pu, Th)O_{2-x}$ in terms of oxygen potential [45]. The $(Pu, Th)O_{2-x}$ is, therefore, analyzed by the chemical thermodynamic method to obtain thermodynamic data for the interaction between PuO_2 and ThO_2.

There are no data for the oxygen potentials of $(RE, Th)O_{2-x}$, $(Eu, Th)O_{2-x}$, $(Ce, Th)O_{2-x}$, $(Th, Zr)O_2$ nor $(Am, Th)O_{2-x}$. The oxygen potentials

for such systems are temporarily assumed to be expressed by ideal solid solutions between ThO_2 and oxides of the solute. This assumption is inferred from the fact that ThO_2 has its unique stable valence states of tetravalence unless the temperature is extremely high, which, however, is not the case for U. Curium is included in the Am elemental group, since CmO_2 is very instable and the oxygen potential of CmO_{2-x} is extremely high, as it is for AmO_{2-x} [46–48]. The largest elemental group is that of the RE elements [25]. The cerium elemental group contains Pr, in addition to Ce itself. Although oxygen potentials for $(Pr,U)O_{2-x}$ are reported to be higher than those of $(U,Ce)O_{2-x}$ [49,50], similar valence states for both elements and phase relations [51] suggest that Pr should be treated as a member of the Ce elemental group.

Europium forms an individual elemental group because of the different aspect of its valence state from the other RE elements; i.e., variable valence from divalent to trivalent. Actually, the oxygen potential of $(Eu,U)O_{2-x}$ shows completely different aspects from those of $(RE,U)O_{2-x}$ [52–54], especially in the O/M ratio where a steep increase of oxygen potential occurs. Thus the stoichiometry (O/M = 2.0) for $(RE,U)O_{2-x}$ can be contrasted to hypostoichiometry for $(Eu,U)O_{2-x}$. Since there are no thermodynamic data for $(Eu,U)O_{2-x}$, a chemical thermodynamic analysis of this system was also carried out.

Once the metal and oxygen balances in the burnup fuel matrix phase are calculated, the oxygen potential of the fuel matrix phase can be estimated by the chemical thermodynamic method with the thermodynamic data of the components. Calculations were made by the SOLGASMIX-PV code [55], in which the Gibbs energy minimization is performed. Thermodynamic data for all components were introduced and the oxygen potentials were calculated as a function of O/M ratio and burnup.

2.4. Chemical thermodynamic analyses of $(Eu, U)O_{2-x}$ and $(Pu, Th)O_{2-x}$

In the chemical thermodynamic analysis of $(Eu,U)O_{2-x}$, the shift of the O/M ratio for the steepest change of the oxygen potential was taken into consideration by adopting appropriate mass parameters. The representation procedure is as follows: first, $[Eu_aO_b]$, $[UO_2]$ and $[Eu_{6c}U_{10c}O_{31c}]$ were considered as mass parameters for $(Eu,U)O_{2-x}$. This set of mass parameters was inferred from the RE-doped UO_2 systems, which introduced sesquioxide that has a relationship of $b = 3/2a$ and a complex oxide between U and RE, such as for $[Ln_{2/3}U_{2/3}O_{8/3}]$ [26]. Although there are several complex oxides between U and Eu, such as $EuUO_3$ [56], the mass parameter was assumed. This composition was decided on the basis of the shift of the O/M ratio for the steepest change of the oxygen potential in the $(Eu,U)O_{2-x}$ system. Using these mass parameters, the gas–solid reaction can be written with the slope s of the oxygen partial pressure versus deviation from stoichiometry, as follows:

$$s[Eu_aO_b] + 10[UO_2] + (O_2) \leftrightarrow [Eu_{6c}U_{10c}O_{31c}]. \quad \{2\}$$

For simplicity, no interactions between the mass parameters were considered. Equations relating T and x from the current methodology can be reduced to a simple expression, as explained in Ref. [22]:

$$\ln(p^*_{O_2}) = A + B/T - \frac{12}{11a - 6b} \cdot \ln(x), \quad (3)$$

where A and B are constants, s replaces the coefficient for the last term of the right side of Eq. (3). A total of 23 points of experimental oxygen potential data were taken for the analysis, which were derived from the graphs of Refs. [52,53] by a digital technique. The analysis gave a scattering of slope from less than 1 up to 6. This scattering of the slope is attributable to the relatively small number of data points. A number of analyses with various a, b and c values were, therefore, carried out. Finally, the best representative case was obtained. The Gibbs energy relation for equilibrium Reaction {2} with the best representative parameters can, thus, be written as

$$RT\ln(p^*_{O_2}) = \Delta\overline{G}[Eu_6U_{10}O_{31}] - 3\Delta\overline{G}[Eu_2O_3] - 10\Delta\overline{G}[UO_2]. \quad (4)$$

The standard Gibbs energies of formation for each mass parameter were obtained by the least square fitting of Eq. (4) to the experimental oxygen potential data. Thermodynamic data for $[Eu_2O_3]$ were retrieved from Ref. [41]. The obtained thermodynamic data are shown in Table 3 together with those used for the representation of the burnup fuel matrix phase.

For $(Pu,Th)O_{2-x}$ analysis, the oxygen potential data of $(Pu_yTh_{1-y})O_{2-x}$ with y of 0.25 and 0.35 at 1273, 1373 and 1473 K reported by Woodley et al. [45] were used. The mass parameters $[PuO_2]$, $[Pu_{4/3}O_2]$ and $[ThO_2]$, whose thermodynamic data have been obtained [24,42], and a newly introduced

first term interaction between $[PuO_2]$ and $[ThO_2]$ were considered. The gas–solid reaction for the system is the same as Reaction {1}. The analytical procedure is the same as that for $(Eu,U)O_{2-x}$. A total of 43 points of experimental oxygen potential data were analyzed by a method similar to that of the $(Eu,U)O_{2-x}$ case. The obtained interaction energy between $[PuO_2]$ and $[ThO_2]$ is also shown in Table 3. The interaction energy is rather small, indicating a weak interaction between the two. The interaction energy between $[AmO_2]$ and $[ThO_2]$ was assumed to be the same as that between $[PuO_2]$ and $[ThO_2]$ for the present evaluation. This assumption was inferred from the following qualitative consideration: there are no thermodynamic data for the solid solution of $(Am,Th)O_{2-x}$. Hence, very close ionic radii between Pu- and Am-oxides for both tetravalent and trivalent cations [57] might lead to similar magnitudes of the interactions of PuO_2 and AmO_2 with ThO_2, since interatomic potentials are a function of interatomic distance. Actual determination of the oxygen potential for $(Am,Th)O_{2-x}$ is, however, needed for more accurate evaluation.

2.5. Results

Fig. 2 shows the variation of the O/M ratio and oxygen potential of $(Am_{0.3}Th_{0.70})O_{2-x}$ with initial O/M = 1.87 at 1473 K. It is seen that both the oxygen potential and O/M ratio decrease with the increase of burnup. The high oxygen potential at the beginning of burnup is of note. The reason is as follows: in the case of 30% of Am inclusion, the initial O/M ratio becomes 1.85 on the condition that all Th are tetravalent and all Am are trivalent. This O/M ratio is the lower limit for the non-stoichiometric single fluorite phase (lower limit O/M ratio) because metal precipitates can appear below this O/M ratio by a shortage of oxygen. Similarly, the lower limit O/M ratio is assigned to the burnup $(Am,Th)O_{2-x}$ by assuming the lowest valence states for each component metal in the oxide. Since the O/M ratio decreases with the increase of burnup, a host phase with an initially low O/M ratio, which is close to the lower limit O/M ratio, can result in the appearance of metal precipitates as burnup increases. This decrease of O/M ratio is attributable to aspects of the oxygen balance in the ThO_2-based oxide fuel that are different from those in UO_2-based fuels. As the main fission source in this fuel is trivalent Am rather than tetravalent U or Pu in the case of standard UO_2-based oxide fuels, oxygen shortage occurs with burnup. In order to avoid this phenomenon, the initial O/M ratio should be increased. In the present case, an initial O/M = 1.87 was adopted, which was attained by an increase of the tetravalent Am fraction. This caused an extremely high oxygen potential in the initial stage of the burnup, as is seen in Fig. 2.

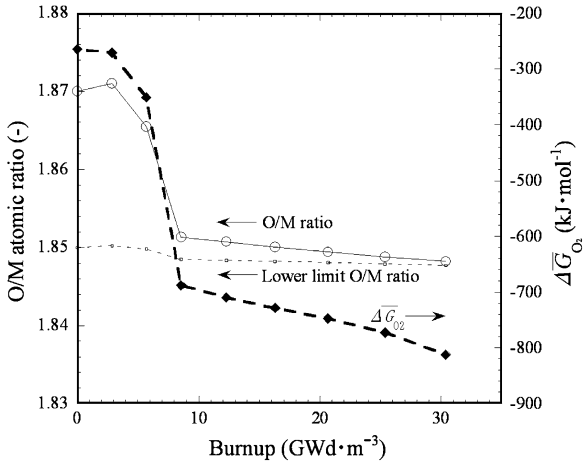

Fig. 2. Variation of the O/M ratio and oxygen potential of $(Am_{0.3}Th_{0.70})O_{2-x}$ with an initial O/M = 1.87 at 1473 K.

3. Discussion

Although the Mo-IM can get surplus oxygen even in the case of $(Am_{0.3}Th_{0.70})O_{2-x}$, the oxygen potential should be suppressed to as low a level as possible. Alternative ideas for the avoidance of both oxygen shortage and initial high oxygen potential at the same time are, therefore, needed. It is seen in Fig. 2 that the high oxygen potential caused by the tetravalent Am begins to decrease at a relatively early point in the burnup, namely around a burnup of 9 GWd m^{-3}. This indicates a replacement of tetravalent Am by pentavalent U, which is generated from Th. The oxygen potential due to pentavalent U in the solid solution is much lower than that of tetravalent Am [29]. Therefore, a small amount of depleted U was added to the $(Am,Th)O_{2-x}$ for the effective increase of the initial O/M ratio, which makes a $(Am,U,Th)O_{2-x}$ solid solution as the initial host phase. Fig. 3 shows the variations of the O/M ratio and oxygen potential with 5% of depleted U-added to $(Am,Th)O_{2-x}$, $(Am_{0.3}U_{0.05}Th_{0.65})O_{2-x}$, with an initial O/M = 1.87 at 1473 K. The margin of the O/M ratio between the lower limit and actual

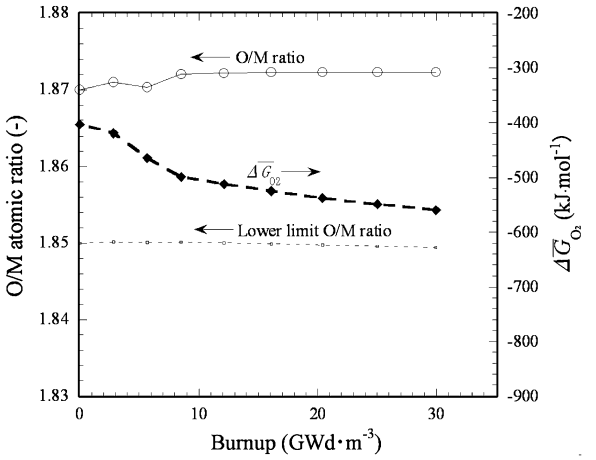

Fig. 3. Variation of the O/M ratio and oxygen potential of $(Am_{0.3}U_{0.05}Th_{0.65})O_{2-x}$ with an initial O/M = 1.87 at 1473 K.

O/M ratios is kept at a constant value throughout the burnup, while that of $(Am_{0.30}Th_{0.70})O_{2-x}$ decreases as was seen in Fig. 2. The oxygen potential of $(Am_{0.3}U_{0.05}Th_{0.65})O_{2-x}$ at the initial stage of burnup, -400 kJ mol^{-1}, is slightly higher than that of MOX, at approximately -500 kJ mol^{-1}. However, the tendency for a decrease in the oxygen potential with burnup can be an advantage over the standard MOX fuel. Fig. 4 shows the variation of the O/M ratio and oxygen potential for a corresponding UO_2-based oxide, namely $(Am_{0.30}U_{0.70})O_{2-x}$, with an initial O/M = 1.87 at 1473 K. Similar tendencies for the variation of the O/M ratio and oxygen potential for $(Am_{0.3}U_{0.05}Th_{0.65})O_{2-x}$ can be seen. From these results, the ThO_2-based oxide seems to display no advantage over UO_2-based oxide for oxygen potential. However, the most significant advantage of the ThO_2-based oxide over the UO_2-based oxide is its better thermal properties, namely higher melting point and thermal conductivity. As an oxide showing such a large deviation from stoichiometry could have much lower thermal properties than those at or near stoichiometry, it should make use of UO_2-based fuel with a low O/M ratio difficult.

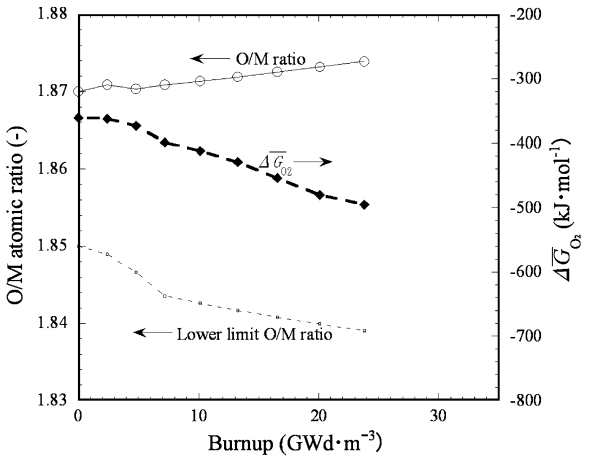

Fig. 4. Variation of the O/M ratio and oxygen potential of $(Am_{0.3}U_{0.7})O_{2-x}$ with an initial O/M = 1.87 at 1473 K.

Another advantage of the depleted U-addition case lies in its nuclear characteristics. The resultant isotopic ratio of U, which is obtained as reprocessed material, can produce a high proliferation resistance compared with a non U-added case, which yields almost pure ^{233}U. The ^{233}U isotopic ratio to that of ^{238}U in the reprocessed material is about 0.77 in the depleted U-addition case. Although this ratio is not low enough to regard the reprocessed U as completely non-weapons-usable [58], the proliferation resistance would effectively be increased by the further optimization of the initial composition of the host phase.

4. Concluding remarks

Prediction of the oxygen potential variation during burnup for the ThO_2-based Am-containing cermet fuel, which consists of $(Am,Th)O_{2-x}$ host phase and molybdenum inert matrix, in a fast reactor was carried out by the chemical thermodynamic method. The oxygen potentials of $(Eu,U)O_{2-x}$ and $(Pu,Th)O_{2-x}$ were analyzed and related thermodynamic data were obtained. These data were useful not only for the present purpose but also for the prediction of UO_2-based fuel. The idea of depleted-U addition can be a novel and an effective way for optimizing the oxygen potential.

It was indicated that this fuel can have several advantages over UO_2-based fuel for MA transmutation in terms of the optimized oxygen potential and a higher thermal performance.

Acknowledgements

The authors are grateful to Mr M. Kato and Mr T. Akashi of A.L.M.T. Corp. for their cooperation to this study.

References

[1] K. Aizawa, Prog. Nucl. Energy 40 (2002) 349.
[2] C. Degueldre, J.M. Paratte, J. Nucl. Mater. 274 (1999) 1.
[3] C. Degueldre, T. Yamashita, J. Nucl. Mater. 319 (2003) 1.

[4] T. Namekawa, K. Kawaguchi, K. Koike, S. Haraguchi, S. Ishii, in: Proc. Int. Conf. GLOBAL2005, Tsukuba, Japan, October 9–13, 2005, paper No. 424.
[5] W. Bartscher, C. Sari, J. Nucl. Mater. 118 (1983) 220.
[6] M. Osaka, I. Sato, T. Namekawa, K. Kurosaki, S. Yamanaka, J. Alloys Comp. 397 (2005) 110.
[7] K. Morimoto, M. Nishiyama, M. Kato, H. Endo, S. Kono, in: Proc. Int. Conf. GLOBAL 2001, Paris, France, September 9–13, 2001.
[8] H.E. Schmidt, C. Sari, K. Richter, J. Less-Common Metals 121 (1986) 621.
[9] T. Hirosawa, K. Tanaka, K. Morimoto, M. Kato, Y. Kihara, T. Ishida, in: Proc. Fall Mtg. Atom. Ene. Soc. Jpn., Kyoto, Japan, September 15–17, 2004, G35, (in Japanese).
[10] M. Osaka, M. Koi, S. Takano, Y. Yamane, T. Misawa, J. Nucl. Sci. Technol. 43 (2006) 367.
[11] S. Nazare, G. Ondracek, F. Thummler, High Temperatures–High Pressures 3 (1971) 615.
[12] J.D.B. Lambert, Metallurgical Soc. Conf, High Temp. Nucl. Fuels Vol. 42, 1966 237.
[13] A. Fernandez, R.J.M. Konings, J. Somers, J. Nucl. Mater. 319 (2003) 44.
[14] L. Donnet, F. Jorion, N. Drin, S.L. Hayes, J.R. Kennedy, K. Pasamehmetoglu, S.L. Voit, D. Haas, A. Fernandez, in: Proc. Int. Conf. GLOBAL2005, Tsukuba, Japan, October 9–13, 2005, paper No. 258.
[15] K. Mayer, B. Kanellakopoulos, J. Naegele, L. Koch, J. Alloys. Comp. 213&214 (1994) 456.
[16] M. Osaka, S. Miwa, H. Yoshimochi, K. Tanaka, K. Kurosaki, S. Yamanaka, Recent Advances in Actinide Science, (2007), p. 406.
[17] K. Bakker, E.H.P. Cordfunke, R.J.M. Konings, R.P.C. Schram, J. Nucl. Mater. 250 (1997) 1.
[18] M. Lung, O. Gremm, Nucl. Eng. Des. 180 (1998) 133.
[19] H. Kleykamp, J. Nucl. Mater. 275 (1999) 1.
[20] Hj. Matzke, V.V. Rondinella, T. Wiss, J. Nucl. Mater. 274 (1999) 47.
[21] J. Wallenius, J. Nucl. Mater. 320 (2003) 142.
[22] T.B. Lindemer, T.M. Besmann, J. Nucl. Mater. 130 (1985) 473.
[23] O. Redlich, A.T. Kister, Ind. Eng. Chem. 40 (1948) 345.
[24] T.M. Besmann, T.B. Lindemer, J. Nucl. Mater. 130 (1985) 489.
[25] T.B. Lindemer, J. Brynestad, J. Am. Ceram. Soc. 69 (1986) 867.
[26] T.B. Lindemer, A.L. Sutton, J. Am. Ceram. Soc. 71 (1988) 553.
[27] C. Thiriet, R.J.M. Konings, J. Nucl. Mater. 320 (2003) 292.
[28] T.B. Lindemer, CALPHAD 10 (1986) 129.
[29] M. Osaka, K. Kurosaki, S. Yamanaka, J. Alloys Comp. 428 (2007) 355.
[30] A.G. Croff, Oak Ridge National Laboratory report, ORNL-TM-7175, 1980.
[31] K. Suyama, J. Katakura, Y. Ohkawachi, M. Ishikawa, Japan Atomic Energy Research Institute report, JAERI-Data/Code 99-003, 1999, (in Japanese).
[32] T. Mizuno, T. Ogawa, M. Naganuma, T. Aida, in: Proc. Int. Conf. GLOBAL2005, Tsukuba, Japan, October 9–13, 2005, paper No. 434.
[33] M. Ugajin, T. Shiratori, K. Shiba, J. Nucl. Mater. 84 (1979) 26.
[34] M. Ugajin, K. Shiba, J. Nucl. Mater. 91 (1980) 227.
[35] M. Ugajin, K. Shiba, J. Nucl. Mater. 105 (1982) 211.
[36] I. Sato, H. Furuya, K. Idemitsu, T. Arima, K. Yamamoto, M. Kajitani, J. Nucl. Mater. 247 (1997) 46.
[37] C. Keller, U. Berndt, H. Engerer, L. Leitner, J. Solid State Chem. 4 (1972) 453.
[38] M.D. Mathews, B.R. Ambekar, A.K. Tyagi, J. Alloys Comp. 386 (2005) 234.
[39] K. Une, M. Oguma, J. Nucl. Mater. 118 (1983) 189.
[40] K. Une, M. Oguma, J. Nucl. Mater. 115 (1983) 84.
[41] E.H.P. Cordfunke, R.J.M. Konings, Thermochemical Data for Reactor Materials and Fission Products, North-Holland, Amsterdam, 1990.
[42] S. Peterson, C.E. Curtis, Thorium ceramics data manual volume I – oxides, Oak Ridge National Laboratory report, ORNL-4503, 1970.
[43] R.E. Woodley, J. Nucl. Mater. 74 (1978) 290.
[44] R.P.C. Schram, J. Nucl. Mater. 344 (2005) 223.
[45] R.E. Woodley, J. Nucl. Mater. 96 (1981) 5.
[46] T.L. Felmlee, B.G. Hyde, C.H. Randall, J. Solid State Chem. 5 (1972) 286.
[47] W.C. Mosley, J. Inorg. Nucl. Chem. 34 (1972) 539.
[48] T.D. Chikalla, L. Eyring, J. Inorg. Nucl. Chem. 31 (1969) 85.
[49] A.J. Freeman, C. KellerHandbook on the Physics and Chemistry of the Actinides, Vol. 6, North-Holland, Amsterdam, 1991.
[50] T. Yamashita, T. Fujino, Proc. Annual mtg. Atom. Ene. Soc. Jpn., Osaka, Japan, 4–6, April, 1989, J3, (in Japanese).
[51] H. Tagawa, T. Fujino, J. Atom. Ene. Soc. Jpn. 22 (1980) 871 (in Japanese).
[52] T. Fujino, N. Sato, K. Yamada, S. Nakama, K. Fukuda, H. Serizawa, T. Shiratori, J. Nucl. Mater. 265 (1999) 154.
[53] T. Fujino, K. Ouchi, Y. Mozumi, R. Ueda, H. Tagawa, J. Nucl. Mater. 174 (1990) 92.
[54] T. Fujino, N. Sato, K. Yamada, S. Nakama, K. Fukuda, H. Serizawa, T. Shiratori, J. Nucl. Mater. 297 (2001) 332.
[55] G. Eriksson, Chemica Scripta 8 (1975) 100.
[56] U. Berndt, R. Tanamas, C. Keller, J. Solid State Chem. 17 (1976) 113.
[57] R.D. Shannon, C.T. Prewitt, Acta Cryst. B 25 (1968) 925.
[58] C.W. Forsberg, C.M. Hopper, J.L. Richter, H.C. Vantine, Oak Ridge National Laboratory report, ORNL/TM-13517, 1998.